Structural Chemistry (2024) 35:1075–1083
https://doi.org/10.1007/s11224-023-02249-2

RESEARCH

Syntheses, crystal structures, spectroscopic and thermal properties of 3D heteronuclear coordination polymers with 4-ethylpyridine and cyanide ligands

Seray Kekeç[1] · Güneş Süheyla Kürkçüoğlu[1] · Okan Zafer Yeşilel[2] · Onur Şahin[3]

Received: 25 August 2023 / Accepted: 23 October 2023 / Published online: 4 November 2023

Abstract

Three new hexacyanometallate(III) complexes, namely $\{[Cd_3(4epy)_{12}Cr_2(\mu\text{-}CN)_6(CN)_6]\bullet 4H_2O\}_n$ (**1**), $\{[Cd_3(4epy)_{12}Fe_2(\mu\text{-}CN)_6(CN)_6]\bullet 4H_2O\}_n$ (**2**) and $\{[Cd_3(4epy)_{12}Co_2(\mu\text{-}CN)_6(CN)_6]\bullet 4H_2O\}_n$ (**3**), were synthesized by using 4-ethylpyridine (4epy) ligand and characterized by spectral (FT-IR and Raman), crystallographic (SC-XRD and PXRD), thermal and elemental analyses techniques. Single crystal studies have shown that heterometallic complexes **1–3** form 3D polymers. Each M ion [M = Cr(III) in **1,** Fe(III) in **2** and Co(III) in **3**] is coordinated by six carbon atoms from cyanide ligands and adjacent metal ions are bridged by cyanide ligands to generate $[Cd_6M_6(CN)_{12}]$ clusters. Each Cd(II) ion is coordinated by four nitrogen atoms from 4epy ligands and two nitrogen atoms from cyanide ligands to distorted octahedral coordination geometry. In addition, thermal (TG/DTA) properties of the complexes were investigated. Powder X-ray diffraction (PXRD) patterns of the complexes were recorded to control the phase purities.

Keywords Hexacyanochromate(III) · Hexacyanoferrate(III) · Hexacyanocobaltate(III) · 4-ethylpyridine · Cadmium(II) · 3D · Coordination polymers

Introduction

Heteronuclear coordination polymers are extended structures formed by the repeated coordination of two or more different metal ions with bridging ligands. These polymers are fascinating because they combine the characteristics of coordination complexes with the advantages of extended networks, such as crystallinity and tunable porosity. They have gained significant attention in materials science and catalysis due to their unique properties and potential applications [1–6]. The formation of heteronuclear coordination polymers typically involves the coordination of metal ions with polydentate ligands that can simultaneously bind to multiple metal centers, bridging them together. The coordination between different metal ions and bridging ligands results in the formation of 1D, 2D or 3D networks depending on the connectivity of the metal centers [5, 7–12]. Coordination polymers with hexacyanometallates, often referred to as hexacyanometallate-based coordination polymers, are a class of compounds where metal ions are bridged by hexacyanometallate(III) ions, ($[M(CN)_6]^{3-}$), to form extended polymeric structures. These coordination polymers have a repeating unit consisting of metal ions and hexacyanometallate ligands, leading to one-dimensional (1D), two-dimensional (2D), or three-dimensional (3D) networks depending on the coordination geometry and connectivity of the metal centers [8, 13–15]. In the literature, it has been stated that inorganic extra framework anions $[Cr(CN)_6]^{3-}$, $[Fe(CN)_6]^{3-}$ and $[Co(CN)_6]^{3-}$ generally provide a very common topology [16].

In our previous studies, we reported hexacyanometallate(III) complexes [8, 13, 15]. The first is $[Cd(tren)(Htren)][Cr(CN)_6]\bullet 2H_2O$ complex synthesized with tris(2-aminoethyl)amine (tren) ligand [15], the other is with 2-(hydroxymethyl)pyridine (hmpy) ligand $[Cd_6(hmpy)_{12}Fe_2(\mu\text{-}CN)_8(CN)_4Fe_2(\mu\text{-}CN)_4(CN)_8]$,

✉ Güneş Süheyla Kürkçüoğlu
gkurkcuo@ogu.edu.tr

1 Faculty of Science, Department of Physics, Eskişehir Osmangazi University, TR-26040 Eskişehir, Turkey

2 Faculty of Science, Department of Chemistry, Eskişehir Osmangazi University, TR-26040 Eskişehir, Turkey

3 School of Health, Department of Occupat Health & Safety, Sinop University, TR-57000 Sinop, Turkey

$[Cd_3(hmpy)_6Co_2(\mu\text{-}CN)_6(CN)_6]$ and $[Zn(hmpy)_2Zn_2(hmpy)_2Co_2(\mu\text{-}CN)_8(CN)_4]_n$ [13], and finally is with 4-(2-aminoethyl)pyridine (4aepy) ligand $\{[Cu(H_2O)(\mu\text{-}4aepy)Cu(\mu\text{-}4aepy)_2Cu(\mu\text{-}4aepy)Co_2(\mu\text{-}CN)_6(CN)_6]\cdot 3H_2O\}_n$, $(NH_4)[Cd(\mu\text{-}4aepy)_2Co(\mu\text{-}CN)_2(CN)_4]_n$ and $(NH_4)[Cd(\mu\text{-}4aepy)_2Fe(\mu\text{-}CN)_2(CN)_4]_n$ [8]. As part of our ongoing research, in this study, three new 3D heteronuclear complexes, $\{[Cd_3(4epy)_{12}Cr_2(\mu\text{-}CN)_6(CN)_6]\bullet 4H_2O\}_n$ (**1**), $\{[Cd_3(4epy)_{12}Fe_2(\mu\text{-}CN)_6(CN)_6]\bullet 4H_2O\}_n$ (**2**) and $\{[Cd_3(4epy)_{12}Co_2(\mu\text{-}CN)_6(CN)_6]\bullet 4H_2O\}_n$ (**3**), were synthesized using 4-ethylpyridine (4epy) ligand and hexacyanometalate(III) complex ions. The structures of the complexes were defined by vibrational (FT-IR and Raman) spectroscopy, crystallographic (SC-XRD and PXRD).

Experimental

Materials and methods

Cadmium acetate dihydrate ($Cd(CH_3COO)_2\bullet 2H_2O$, Acros, 99%), potassium hexacyanochromate(III) ($K_3[Cr(CN)_6]$, Merck, 99%), potassium hexacyanoferrate(III) ($K_3[Fe(CN)_6]$, Merck, 99%), potassium hexacyanocobaltate(III) ($K_3[Co(CN)_6]$, Acros, 95%), 4-ethylpyridine (C_7H_9N, thermoscientific, 98%), ammonia solution (NH_4OH, Merck, 25%) and ethanol (C_2H_5OH, Merck) were purchased from commercial sources and were used as received. Elemental analyses results were taken on LECO CHNS-932 analyzer for C, H and N. FT-IR spectra were recorded with a Perkin Elmer 100 FT-IR spectrometer (calibrated using polystyrene and CO_2 bands) with ATR (Atenuated Total Reflection) at 4000–250 cm^{-1} (4 cm^{-1} resolution). Raman spectra were recorded in the Bruker Senterra Dispersive Raman instrument at the range of 4000–250 cm^{-1} using 785 nm laser excitation. Powder X-ray diffraction (PXRD) patterns were obtained from a Panalytical EMPYREAN X-ray diffraction instrument operating at 40 kV and 30 mA with Cu-Kα radiation (λ = 1.5406 nm). The Perkin Elmer Diamond TG/DTA Thermal Analyzer was used at a heating rate of 10 °C/min. in a temperature range of 30–1000 °C in a static atmosphere to record the TG, DTG and DTA curves.

Single crystal analyses

Suitable crystals of **1–3** were selected for data collection which was performed on a Bruker diffractometer equipped with a graphite-monochromatic Mo-K_α radiation at 296 K. The refinements of the disordered groups (most carbon atoms in ethyl groups) were made anisotropicaly using PART, EADP and ISOR restrictions. This disorder was modelled as two different orientations as two groups [first group = A and second group = B], with occupancy factors of 0.486(4) and 0.514(4) in **1**, 0.495(5) and 0.505(5) in **2** and 0.579(4) and 0.421(4) in **3**, respectively. During the refinement of the complexes **1–3**, electron density peaks were located that were believed to be highly disordered water molecules. Attempts made to model the water molecule were not successful. The SQUEEZE option in PLATON [25] indicated there was a large solvent cavity of 942 $Å^3$ in **1**, 786 $Å^3$ in **2** and 789 $Å^3$ in **3**. In the final cycles of refinement, this contribution of 205 electrons in **1**, 331 electrons in **2** and 168 electrons in **3** to the electron density was removed from the observed data and the hkl intensities were modified accordingly. We used these procedures for our analyses: solved by direct methods; SHELXS-2013 [17]; refined by full-matrix least-squares methods; SHELXL-2013 [18]; data collection: Bruker APEX2 [19]; molecular graphics: MERCURY [20]; solution: WinGX [21]. The crystal structure determinations and complete details of the data collected can be observed in (Table 1).

Synthesis and characterization

1 mmol of $K_3[M(CN)_6]$ [M = Cr (0.325 g), Fe (0.329 g) or Co (0.332 g)] was dissolved in [4:1] distilled water/ammonium hydroxide mixture. While the solution was stirred, 1 mmol of $Cd(CH_3COO)_2\bullet 2H_2O$ (0.266 g) dissolved in 20 mL distilled water was added slowly to the mixture. The resulting mixture was stirred on a magnetic stirrer for 15 min. To this obtained mixture, 4 mmol of 4epy (0.428 g) ligand dissolved in distilled water/ethanol ratio [1:1] was added dropwise, then the resulting complex was stirred at 50 °C for 5 h, filtered and left to crystallize at room temperature. Within a week or two, crystals formed (Scheme 1).

In this way, complex **1** $\{[Cd_3(4epy)_{12}Cr_2(\mu\text{-}CN)_6(CN)_6]\bullet 4H_2O\}_n$ has colourless crystals. The yield of the synthesized chemical is 42%. (based on $Cd(CH_3COO)_2\bullet H_2O$) Anal. Calcd. for $C_{96}H_{116}Cd_3Cr_2N_{24}O_4$ (**1**) (MW = 2111.32 g mol^{-1}): C 51.00, H 5.13, N 15.40%; found C 51.70, H 5.63, N 15.65%. Complex **2** $\{[Cd_3(4epy)_{12}Fe_2(\mu\text{-}CN)_6(CN)_6]\bullet 4H_2O\}_n$ has yellow crystals. The yield of the synthesized chemical is 46% (based on $Cd(CH_3COO)_2\bullet 2H_2O$) Anal. Calcd. for $C_{96}H_{116}Cd_3Fe_2N_{24}O_4$ (**2**) (MW = 2119.02 g mol^{-1}): C 50.60, H 5.10, N 15.90%; found C 50.50, H 5.61, N 15.60%. Complex **3** $\{[Cd_3(4epy)_{12}Co_2(\mu\text{-}CN)_6(CN)_6]\bullet 4H_2O\}_n$ has colourless crystals. The yield of the synthesized chemical is 53% (based on $Cd(CH_3COO)_2\bullet 2H_2O$) Anal. Calcd. for $C_{96}H_{116}Cd_3Co_2N_{24}O_4$ (**3**) (MW = 2125.18 g mol^{-1}): C 46.80, H 4.90, N 13.90%; found C 46.35, H 4.60, N 13.55%.

Table 1 Crystal data and structure refinement parameters for complexes **1–3**

Crystal data	**1**	**2**	**3**
CCDC	**2252864**	**2252866**	**2252865**
Crystal data			
Empirical formula	$C_{96}H_{116}Cd_3Cr_2N_{24}O_4$	$C_{96}H_{116}Cd_3Fe_2N_{24}O_4$	$C_{96}H_{116}Cd_3Co_2N_{24}O_4$
Formula weight g/mol	2111.32	2119.02	2125.18
Crystal system	Trigonal	Trigonal	Trigonal
Space group	*R-3:H*	*R-3:H*	*R-3:H*
a (Å)	38.3864(17)	38.252(4)	38.096(2)
c (Å)	20.7679(16)	20.347(3)	20.2125(16)
V (Å^3)	26502(3)	25784(7)	25405(4)
Z	9	9	9
D_c (g cm^{-3})	1.191	1.228	1.250
μ (mm^{-1})	0.76	0.85	0.90
Data collection			
$\theta_{min\text{-}max}$ (°)	2.4–26.7	1.1–28.2	2.4–28.3
Measured refls	112035	143857	174950
Independent refls	12488	14150	13980
R_{int}	0.085	0.062	0.074
Refinement			
S	1.03	1.18	1.14
R1/wR2	0.062/0.161	0.069/0.189	0.067/0.166
$\Delta\rho_{max}/\Delta\rho_{min}$ (eÅ^{-3})	0.55/-0.48	1.10/-0.70	1.24/-0.67

Results and discussion

X-ray diffraction studies

The crystallographic data of the complexes, the selected bond lengths and angles, and the hydrogen bond geometries of the complexes are given in Tables 1, 2 and 3, respectively. The purities of complexes **1**–**3** were validated through the utilization of the complexes PXRD patterns (Fig. S1). Based on the comparison between the calculated data from the SC-XRD powder patterns collected with the help of the Mercury CSD software package and the experimental data, the result was both similar approving the purity of the crystals.

Structural description of 1–3

The single crystal X-ray study shows that the heterometallic complexes **1–3** form 3D polymers. Crystallographic analyses showed that complexes **1**–**3** with space group R-3 are very similar. Complexes **1**–**3** show isostructural features. Additionally, **1**–**3** are isotypic with heterometallic MOFs reported in the literature [22]. The asymmetric unit of the complexes **1–3** consists of one and half Cd(II) ions, one M ion [M = Cr(III) in **1,** Fe(III) in **2** and Co(III) in **3**], six 4epy ligands, six cyanide ligands and two non-coordinated water molecules (Fig. 1). In **1–3**, each Cd(II) ion is coordinated by four nitrogen atoms from 4epy ligands and two nitrogen atoms from cyanide ligands (Table 2). In **1–3**, the position of Cd2 atom coincides with the location of the symmetry centre. Each M ion [M = Cr(III) in **1,** Fe(III) in **2** and Co(III) in **3**] is coordinated by six carbon atoms from cyanide ligands. M(III)-C bond lengths**,** 2.048(5), 2.071(5), 2.054(7), 2.051(5), 2.067(5) and 2.071(7) in **1**, 1.936(4), 1.955(7), 1.940(5), 1.917(4), 1.947(7) and 1.949(5) in **2** and 1.902(5), 1.905(4), 1.899(6), 1.878(4), 1.892(6) and 1.896(4) in **3**. In **1**–**3**, the coordination spheres of all ions are octahedral coordination geometry. The ions are bridged by cyanide ligands to generate $[Cd_6M_6(CN)_{12}]$ metalloligands [M = Cr(III) in **1,** Fe(III) in **2** and Co(III) in **3**], with the Cd(II)•••M separations are 5.437 and 5.441 Å in **1,** 5.341 and 5.344 Å in **2** and 5.274 and 5.310 Å in **3**. Adjacent these metalloligands are joined by cyanide ligands, generating

$$2K_3[M(CN)_6]\,(s) + 3Cd(CH_3COO)_2\,(s) + 12(4epy)\,(l) \xrightarrow[NH_4OH\ (5\ mL),\ 50\ ^oC]{Ethanol/water,\ 4h} [Cd_3(4epy)_{12}M_2(\mu\text{-}CN)_6(CN)_6]\cdot 4H_2O\,(s) + 6K(CH_3COO)\,(aq)$$

Scheme 1 Synthesis methods of complexes **1–3**

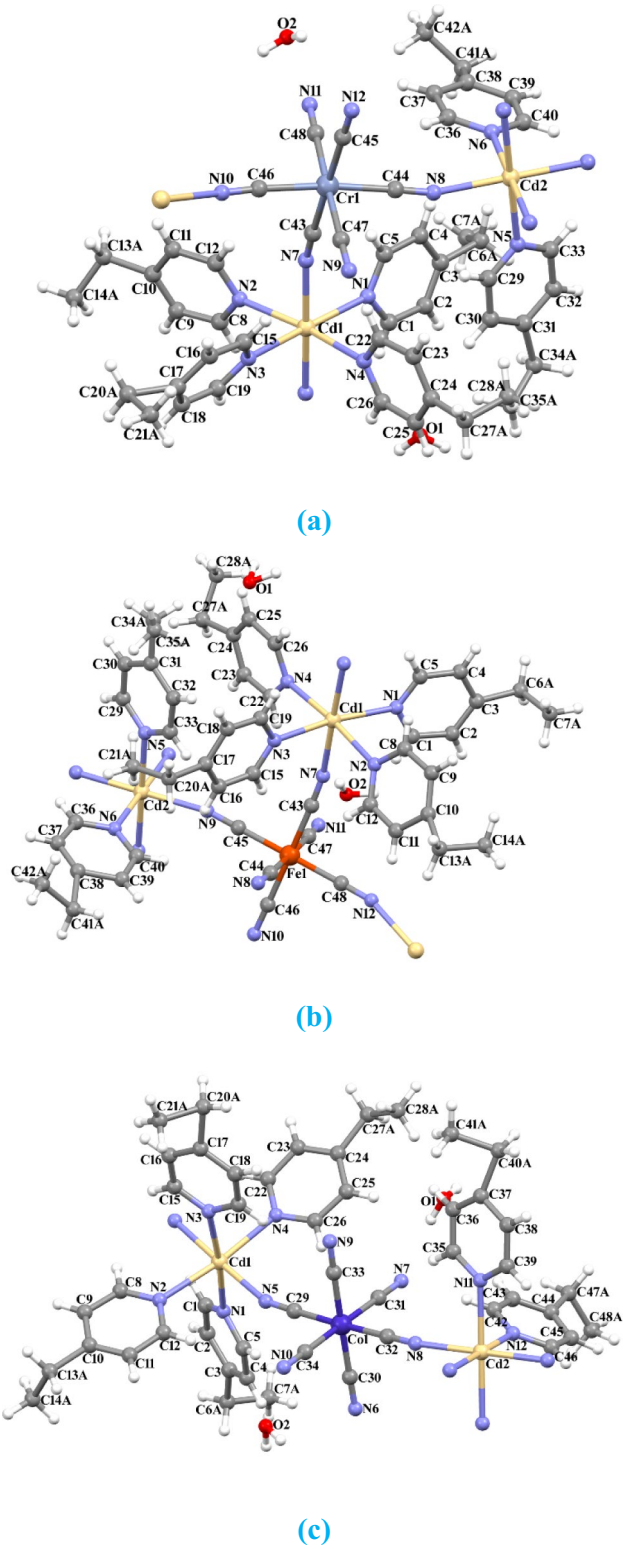

Fig. 1 The molecular structures of 1 **(a)**, 2 **(b)** and 3 **(c)** showing the atom numbering schemes. Some carbon atoms in the ethyl groups of 4epy ligands are disordered. For the sake of clarity, only in "A" occupied positions are shown

Table 2 Selected bond distances for complexes **1–3** (Å, °)

Complex **1**					
Cd1-N1	2.372(4)	Cd1-N2	2.382(4)	Cd1-N3	2.414(4)
Cd1-N4	2.408(4)	Cd1-N7	2.308(4)	Cd1-N10^{i}	2.298(4)
Cd2-N5	2.374(4)	Cd2-N6	2.367(5)	Cd2-N8	2.288(4)
Cr1-C43	2.048(5)	Cr1-C44	2.051(5)	Cr1-C45	2.067(5)
Cr1-C46	2.071(5)	Cr1-C47	2.071(7)	Cr1-C48	2.054(7)
Complex **2**					
Cd1-N1	2.383(4)	Cd1-N2	2.429(4)	Cd1-N3	2.408(4)
Cd1-N4	2.367(4)	Cd1-N7	2.310(4)	Cd1-N12^{i}	2.298(4)
Cd2-N5	2.369(4)	Cd2-N6	2.368(6)	Cd2-N9	2.315(4)
Fe1-C43	1.949(5)	Fe1-C44	1.947(7)	Fe1-C45	1.917(4)
Fe1-C46	1.940(5)	Fe1-C47	1.955(7)	Fe1-C48	1.936(4)
Complex **3**					
Cd1-N1	2.360(4)	Cd1-N2	2.401(4)	Cd1-N3	2.399(4)
Cd1-N4	2.388(4)	Cd1-N5	2.310(4)	Cd1-N10^{i}	2.319(4)
Cd2-N8	2.318(4)	Cd2-N12	2.362(4)	Cd2-N11	2.367(5)
Co1-C29	1.905(4)	Co1-C30	1.899(6)	Co1-C31	1.902(5)
Co1-C32	1.878(4)	Co1-C33	1.892(6)	Co1-C34	1.896(4)

Symmetry codes: (i) y-1/3, -x + y + 1/3, -z + 4/3 for **1,** (i) x–y + 2/3, x + 1/3, -z + 4/3 for **2**; (i) x–y + 1, x, -z + 1 for **3**

3D coordination polymer (Fig. 2). The 3D coordination polymers are also supported by intermolecular O–H•••N hydrogen bonds (Table 3). In the literature, intermolecular O–H•••N hydrogen bonds are seen in many studies [23–28].

Spectral studies

FT-IR spectra of the complexes are shown in Fig. 3 and Raman spectra are shown in Fig. 4. The vibrational bands of the complexes and the 4epy are given in Table 4 [29–31]. Symmetrical and asymmetrical ν(OH) stretching vibrations of the complexes were observed in the region of 3550–3200 cm^{-1}, and δ(OH) bending vibrations were observed in the range of 1630–1600 cm^{-1} wavenumbers [32]. According to this, asymmetric and symmetrical ν(OH) stretching vibration wavenumbers were found to be 3370 cm^{-1} for **1**, 3346 cm^{-1} for **2**, and 3378 cm^{-1} for **3**. In addition, δ(OH) bending vibrations have wavenumber values of 1630 cm^{-1} for **1**, 1630 cm^{-1} for **2** and 1624 cm^{-1} for **3**.

When the nitrogen atom in the pyridine ring participates in the coordination, significant shifts can be observed in the ring vibration wavenumbers relative to 4epy [29, 30]. Vibration bands ν(C = C) and ν(C = N) are important bands of pyridine ring. The stretching vibration band ν(C = C) found at 1561 cm^{-1} in FT-IR spectrum of 4epy is observed at 1555 cm^{-1} and 1544 cm^{-1} for **1**, 1555 cm^{-1} and 1561 cm^{-1} for **2** and 1555 cm^{-1} and 1555 cm^{-1} for **3** in FT-IR and Raman spectra, respectively. The stretching ν(C = N) band

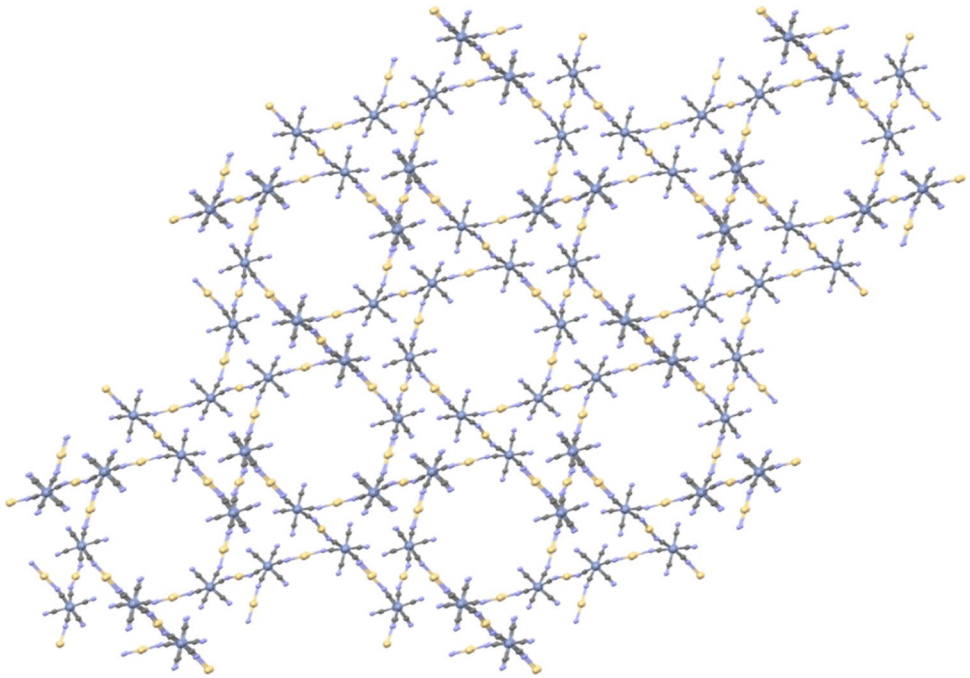

Fig. 2 An infinite 3D coordination polymer in **1–3**. The 4epy ligands and water molecules have been omitted for clarity

is found at 1499 cm^{-1} in FT-IR spectrum of 4epy, while it is observed at 1498 cm^{-1} and 1492 cm^{-1} for **1**, 1501 cm^{-1} and 1492 cm^{-1} for **2** and 1503 cm^{-1} and 1492 cm^{-1} for **3** in FT-IR and Raman spectra, respectively.

The ν(CH) vibrational bands observed in the wavenumber range of 3068–2970 cm^{-1} in FT-IR spectrum of 4epy were found in the wavenumber range of 3079–2970 cm^{-1} in those of the complexes. In aromatic molecules, ν(CH) stretching vibration bands are found in the wavenumber range of 3100–3000 cm^{-1} [33, 34]. Vibrational δ(CH) band is observed at 1316 cm^{-1} in the spectra of 4epy ligand, while it is observed at 1314 cm^{-1} in the complexes **1–3**. In additional, ring stretching ν_{ring} vibrations, which appeared in 4epy at 1600 cm^{-1}, 1559 cm^{-1} and 1497 cm^{-1}, were observed in the complexes at 1613 cm^{-1}, 1555 cm^{-1} and 1498 cm^{-1} in **1**, at 1613 cm^{-1}, 1555 cm^{-1} and 1501 cm^{-1} in **2** and at 1613 cm^{-1}, 1555 cm^{-1} and 1503 cm^{-1} in **3**. These shifts can be observed in the ring vibrations of 4epy, when nitrogen atom in the pyridine ring participates in the coordination. Complexes **1–3** contains cyanide groups and cyanide stretching band is observed in the FT-IR spectra at 2153 cm^{-1} for **1**, 2143 cm^{-1} for **2** and **3**. In Raman spectrum, 2148 cm^{-1} and 2113 cm^{-1} for **1**, 2142 cm^{-1} and 2073 cm^{-1} for **2** and 2171 cm^{-1} and 2142 cm^{-1} for **3**.

The spectral data of complexes and bond lengths of the crystals were examined. According to this, the C43≡N7 and C44≡N8 bond lengths for **1** are found to be 1.147(5) and 1.156(6) Å, respectively. The bridged Cd–N cyanide bond lengths affecting the position of the ν(C≡N) streching band are [Cd1-N7 = 2.315(6) Å, Cd2-N9 = 2.312 Å)], affecting the position of the ν(C≡N) stretching band, are essentially different, which result in one stretching band in the FT-IR spectrum [2153 cm^{-1} for C43≡N7]. For **2**, the bond lengths of C43≡N7 and C45≡N9 are found as 1.138(8) and 1.156(6) Å, respectively. The bridged Cd–N cyanide bond lengths affecting the position of the ν(C≡N) streching band are [Cd1-N7 = 2.315(6) Å, Cd2-N9 = 2.312 Å)], affecting

Table 3 Hydrogen-bond parameters for complexes **1–3** (Å, °)

D-H···A	D-H	H···A	D···A	D-H···A
Complex **1**				
C12—H12···N7	0.93	2.58	3.239(7)	128
O1—H1A···N12^{iv}	0.88	2.46	3.072(8)	126
O1—H1B···N11^{i}	0.85	2.47	3.288(9)	161
O2—H2A···N12^{v}	0.80	2.37	3.065(8)	144
O2—H2B···N11	0.85	2.38	2.900(8)	120
Complex **2**				
C1—H1···N7	0.93	2.56	3.226(7)	129
O1—H1A···N10^{iv}	0.88	2.46	3.073(9)	126
O1—H1B···N11^{i}	0.97	2.31	3.188(10)	151
O2—H2B···N10^{v}	0.88	2.23	3.047(9)	154
Complex **3**				
C22—H22···N10^{i}	0.93	2.55	3.220(7)	129
O1—H1B···N7	0.84	2.21	3.028(8)	167
O1—H1A···N6^{iv}	0.82	2.13	2.917(8)	162
O2—H2B···N7^{v}	0.88	2.29	3.124(9)	158

Symmetry codes: (i) y − 1/3, − x + y + 1/3, − z + 4/3; (iv) x − y + 1/3, x − 1/3, − z + 5/3; (v) − y + 4/3, x − y + 2/3, z − 1/3 for **1**; (i) x − y + 2/3, x + 1/3, − z + 4/3; (iv) y, − x + y + 1, − z + 1; (v) − x + y + 2/3, − x + 4/3, z + 1/3 for **2**; (i) x − y + 1, x, − z + 1; (iv) − x + y + 2/3, − x + 4/3, z + 1/3; (v) − y + 4/3, x − y + 2/3, z − 1/3 for **3**

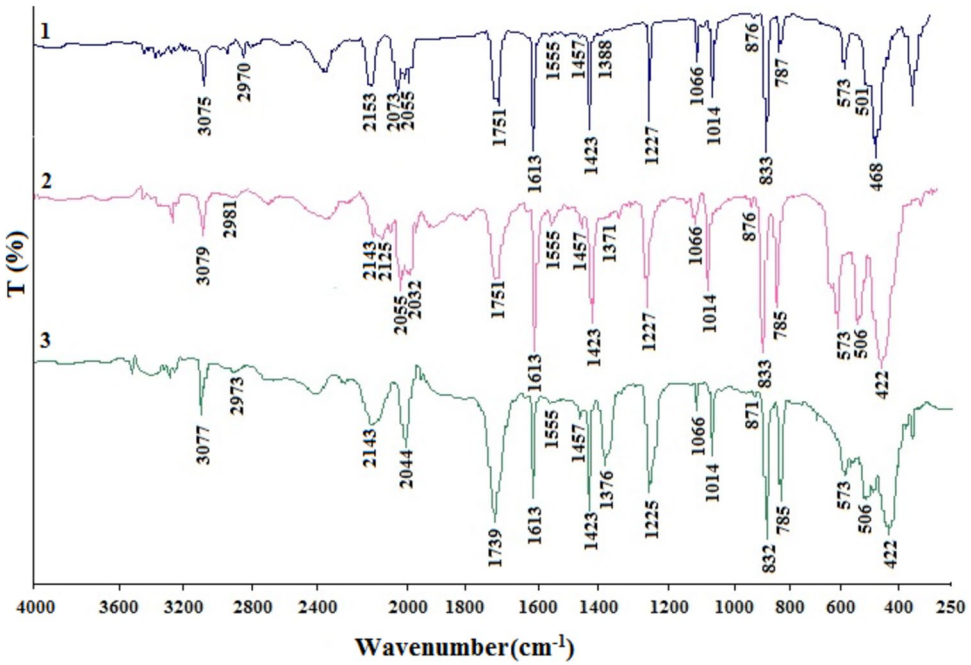

Fig. 3 The FT-IR spectra of complexes **1–3**

the position of the ν(C≡N) stretching band, are essentially different, which result in one stretching band in the FT-IR spectrum [2143 cm^{-1} for C43≡N7]. And for **3**, C29≡N5 and C32≡N8 bond lengths are found to be 1.136(7) and 1.151(7) Å, respectively. The bridged Cd–N cyanide bond lengths that affect the position of the ν(C≡N) streching bands are [Cd1-N5 = 2.313(5) Å, Cd2-N8 = 2.317 Å)], affecting the position of the ν(C≡N) stretching band, are essentially different, which result in one stretching band in the FT-IR spectrum [2143 cm^{-1} for C32≡N8].

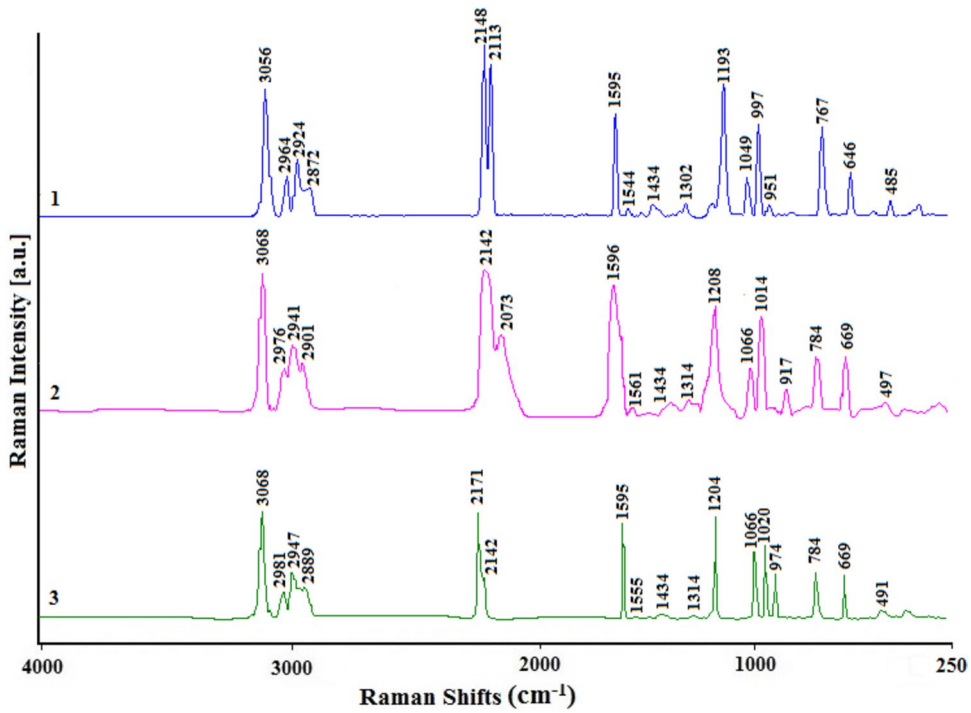

Fig. 4 The Raman spectra of complexes **1–3**

Table 4 The FT-IR and Raman wavenumbers of 4epy in **1–3** (cm^{-1})

Assignments [29–31]	**4epy**	**1**		**2**		**3**	
		FT-IR	Raman	FT-IR	Raman	FT-IR	Raman
ν(CH)	3068 m	3075 m	3056 s	3079 m	3068 s	3077 m	3068 s
ν(CH)	3044 w	3051 vw	3052 vs	3051 vw	3050 vw	3052 vw	3051 sh
ν(CH)	2970 s	2970 vw	2964 m	2981 vw	2976 m	2973 vw	2981 m
$\nu_a(CH_3)$	2935 m	2935 vw	2924 m	2935 vw	2941 m	2935 vw	2947 m
$\nu_a(CH_2)$	2901 w	2909 vw	2925 m	-	2902 m	2904 vw	2911 m
$\nu_s(CH_3)$	2877 m	2866 vw	2872 m	2866 vw	2870 sh	2878 vw	2878 sh
ν(CH)	1988 w	2000 sh	1990 vw	1986 vw	1996 sh	1986 vw	1983 vw
X_{sens}	1933 vw	1959 vw	1939 vw	1966 vw	1934 w	1970 vw	1942 vw
X_{sens}	1791 vw	1791 vw	1788 vw	1791 sh	1802 vw	1793 vw	1793 vw
X_{sens}	1733 w	1751 m	1734 w	1751 m	1731 sh	1739s	1736 vw
ν_{ring}	1600 vs	1613 s	1595 s	1613 s	1596 s	1613 s	1595 s
ν(CC)	1561 m	1555 vw	1544 w	1555 vw	1561 w	1555 vw	1555 vw
ν(CN)	1499 m	1498 vw	1492 vw	1501 vw	1492 vw	1503 vw	1492 vw
$\delta_a(CH_3)$	1449 m	1457 w	1434 w	1457 w	1434 w	1457 w	1434 w
ν_{ring}	1414 vs	1423 s	1436 m	1423 s	1426 m	1423 s	1425 w
$\nu_s(CH_3)$	1376 w	1388 vw	1360 vw	1371 vw	1360 vw	1367 m	1360 vw
δ(CH)	1316 w	1314 vw	1302 vw	1314 vw	1314 vw	1314 vw	1314 vw
ν_t(CH)	1265 w	1273 vw	1239 w	1270 vw	1272 sh	1271 vw	1239 vw
δ(CH)	1219 s	1227 s	1193 s	1227 s	1208 s	1225 s	1204 s
$\nu_r(CH_3)$	1099 w	1101 vw	1098 vw	1090 vw	1106 vw	1089 vw	1090 vw
$\delta(CH)+\nu_{ring}$	1068 m	1066 m	1049 m	1066 m	1066 m	1066 m	1066 m
$\nu_r(CH_3)$	1036 sh	1026 sh	1047 m	1028 sh	1020 m	1038 w	1020 m
Ring breath	994 m	1014 m	997 m	1014 m	1014 m	1014 m	1018 m
γ(CH)	976 sh	979 vw	951 w	978 vw	976 w	987 vw	974 w
γ(CH)	877 vw	876 vw	887 w	876 vw	882 vw	871 vw	876 w
γ(CH)	820 vs	833 vs	818 w	833 vs	828 vw	832 vs	817 vw
$\gamma_{ring}(R_{sens}.)$	776 s	787 m	767 s	785 s	784 m	785 s	784 m
δ(CC)	757 w	758 vw	770 s	762 vw	756 vw	762 w	761 sh
γ_{ring}	720 vw	713 vw	723 w	713 vw	711 vw	713 vw	726 vw
δ_{ring}	670 vw	672 vw	646 m	-	669 m	-	669 m
$\gamma_{ring}(R_{sens}.)$	566 s	573 m	587 w	573 s	576 vw	573 m	575 vw
δ(CC)	515 m	499 m	504 vw	505 s	506 m	517 s	514 vw
$\gamma_{ring}(R_{sens}.)$	490 s	501 m	485 vw	506 m	497 vw	506 m	491 vw

ν stretching, δ deformation, *w* wagging, *t* twisting, *r* rocking, *s* strong, *m* medium, *w* weak, *sh* shoulder, *v* very

Thermal analyses

Thermal analyses of the complexes were taken in a static air atmosphere with a heating rate of 10 °C from 30 °C to 1000 °C and the TG, DTA and DTG curves are shown in Fig. S2. The thermal decomposition of **1–3** proceeds in two stages. In the first stage of complexes **1–3,** the complexes lose four water molecules and twelve 4epy ligands in the temperature range 30–359 °C [found (calcd.)(%) = 60.65 (60.82)] for **1**; 39–374 °C [found (calcd.)(%) = 59.58 (59.68)] for **2** and 38–353 °C [found (calcd.)(%) = 60.55 (60.50) for **3**. The second stage is related to release of twelve cyanide ligands in the temperature range 359–458 °C [found (calcd.)(%) = 14.55 (14.54)] for **1**; 374–491 °C [found (calcd.)(%) = 14.46 (14.48)] for **2**; 353–442 °C [found (calcd.)(%) = 14.30 (14.45)] for **3**. The strong exothermic peak in the last step ($DTA_{max.}$ = 438 °C for **1;** 460 °C for **2** and 409 ºC for **3**) is associated with the combustion of the remaining the organic residue in complexes **1–3**. The final solid products of thermal decompositions, $CdO+Cr_2O_3$ for **1**, $CdO+Fe_2O_3$ for **2** and $CdO+Co_3O_4$ for **3**. The final decomposition products may be Co_3O_4 which converts to CoO above 905 °C for **3**.

Conclusion

In this study, three dimensional heteronuclear complexes were synthesized under similar conditions by using hexacyanometallate(III) (M = Cr, Fe and Co) ions and 4epy ligand. Single crystal X-ray diffraction studies revealed that complexes **1–3** exhibit a 3D framework based on the $[Cd_6M_6(CN)_{12}]$ cluster. In **1–3**, each Cd(II) ion is coordinated by six nitrogen atoms. Complexes 1**–3** exhibit distorted octahedral coordination geometries with the axial positions occupied by two cyanide ligands.

Supplementary Information The online version contains supplementary material available at https://doi.org/10.1007/s11224-023-02249-2.

Acknowledgements The authors acknowledge to Scientific and Technological Research Application and Research Center, Sinop University, Türkiye, for the use of the Bruker D8 QUEST diffractometer.

Author contributions All authors share equally in writing the main manuscript, preparing the figures and the tables.

Funding This work has been financially supported by Eskişehir Osmangazi University, Scientific research Unit [grant no: 2022–2561].

Data availability Data will be available on request.

Declarations

Conflict of interest The authors declare that they have no confict of interest.

References

1. Gupta R, Pachisia S, Gupta R (2023) Supramolecular coordination complexes from metalloligands: Heteronuclear complexes and coordination polymers and their applications in catalysis. Supramol Coord Comp 43–68
2. Blais C, Daiguebonne C, Suffren Y, Bernot K, Calvez G, Le Pollès L (2022) Investigation of intermetallic energy transfers in lanthanide coordination polymers molecular alloys: case study of trimesate-based compounds. Inorg Chem 61(30):11897–11915
3. Hasegawa Y, Shoji S, Kitagawa Y (2022) Luminescent Eu(III)-based coordination polymers for photonic materials. Chem Lett 51(2):185–196
4. Denk A, Kernbichl S, Schaffer A, Kränzlein M, Pehl T, Rieger B (2020) Heteronuclear, monomer-selective Zn/Y catalyst combines copolymerization of epoxides and CO_2 with group-transfer polymerization of Michael-type monomers. ACS Macro Lett 9(4):571–575
5. Mwanza T, Kürkçüoğlu GS, Ünver H, Şahin O, Yeşilel OZ (2022) Synthesis, spectroscopic, structural characterizations, and catalytic properties of cyanide-bridged heteronuclear metal organic frameworks with imidazole. J Solid State Chem 314:123344
6. Liu Q-F, Liu W, Cao Y-P, Dong Y-L, Liu H-M (2017) A new heterometallic coordination polymer: Synthesis, structure, and catalytic property. Inorg Nano-Met 47(1):153–157
7. Kürkçüoğlu GS, Yeşilel OZ, Sayın E, Şahin O (2021) Two-dimensional heteronuclear coordination polymers constructed by cyanide and 3-(2-Aminoethyl)pyridine ligands. J Inorg Organomet Polym Mater 31:112–120
8. Kürkçüoğlu GS, Yeşilel OZ, Kekeç S, Şahin O (2023) Synthesis, crystal structure and spectroscopic investigations of heteronuclear Co(III)/Cu(II), Co(III)/Cd(II) and Fe(III)/Cd(II) 3D coordination polymers with 4-(2-aminoethyl) pyridine. J Mol Struct 1274:134540
9. Majumdar D, Tüzün B, Pal TK, Das S, Bankura K (2022) Architectural view of flexible aliphatic-OH group coordinated hemi-directed Pb(II)-Salen coordination polymer: Synthesis, crystal structure, spectroscopic insights, supramolecular topographies, and DFT perspective. J Inorg Organomet Polym Mater 32(3):1159–1176
10. Ju H, Habata Y, Jung JH, Lee SS (2021) Coordinative networking of thiacalix [4]-bis-monothiacrown-5 with hard, borderline, and soft metal salts via exo-and endo/exo-coordination. Cryst Growth Des 21(12):6992–7001
11. Mondal S, Dastidar P (2020) Zn(II)-coordination polymers with a right- and left-handed twist: Multifunctional metal-organic hybrid for dye adsorption and drug delivery. Cryst Growth Des 20(11):7411–7420
12. Ali A, Muslim M, Neogi I, Afzal M, Alarifi A, Ahmad M (2022) Construction of a 3D metal-organic framework and its composite for water remediation via selective adsorption and photocatalytic degradation of hazardous dye. ACS Omega 7(28):24438–24451
13. Sayın E, Kürkçüoğlu GS, Yeşilel OZ, Şahin O (2021) Unprecedented deca-, penta- and poly- heteronuclear complexes with hexacyanometallates and 2-(hydroxymethyl) pyridine. Polyhedron 210:115535
14. Avila Y, Acevedo-Peña P, Reguera L, Reguera E (2022) Recent progress in transition metal hexacyanometallates: From structure to properties and functionality. Coord Chem Rev 453:214274
15. Kürkçüoğlu GS, Yeşilel OZ, Sayın E, Enönlü E, Şahin O (2020) Synthesis and structural analysis of heteronuclear hexacyanochromate(III) complex with tris(2aminoethyl)amine), $[Cd(tren)(Htren)][Cr(CN)_6]\cdot 2H_2O$. J Mol Struct 1219:128462
16. Alexandrov EV, Virovets AV, Blatov VA, Peresypkina EV (2015) Topological motifs in cyanometallates: From building units to three-periodic frameworks. Chem Rev 115(22):12286–12319
17. Sheldrick GM (2008) A short history of SHELX. Acta Crystallogr Sect A: Found Crystallogr 64(1):112–122
18. Sheldrick GM (2015) SHELXT–Integrated space-group and crystal-structure determination. Acta Crystallogr Sect A: Found Adv 71(1):3–8
19. Package AS (2005) Bruker AXS Inc., 5465. East Cheryl Parkway, Madison, Wisconsin, USA
20. Macrae CF, Sovago I, Cottrell SJ, Galek PT, McCabe P, Pidcock E (2020) Mercury 4.0: From visualization to analysis, design and prediction. J Appl Crystallogr 53(1):226–235
21. Farrugia LJ (2012) WinGX and ORTEP for Windows: An update. J Appl Crystallogr 45(4):849–854
22. Kaneko W, Mito M, Kitagawa S, Ohba M (2008) Interpenetrated three-dimensional $Mn^{II}M^{III}$ ferrimagnets,$[Mn(4dmap)_4]_3[M(CN)_6]_2\cdot 10H_2O$ (M= Cr, Mn): Structures, magnetic properties, and pressure-responsive magnetic modulation. Chem Eur J 14(11):3481–3489
23. Steiner T, Majerz I, Wilson CC (2001) First OHN hydrogen bond with a centered proton obtained by thermally induced proton migration. Angew Chem Int Ed 40(14):2651–2654
24. Ip BC, Shenderovich IG, Tolstoy PM, Frydel J, Denisov GS, Buntkowsky G (2012) NMR studies of solid pentachlorophenol-4-methylpyridine complexes exhibiting strong OHN hydrogen bonds: Geometric H/D isotope effects and hydrogen bond coupling cause isotopic polymorphism. J Phys Chem A 116(46):11370–11387
25. Bertolasi V, Gilli P, Ferretti V, Gilli G (1995) Intermolecular N-H···O hydrogen bonds assisted by resonance. Heteroconjugated

systems as hydrogen-bond-strengthening functional groups. Acta Crystallogr Sect B: Struct Sci 51(6):1004–1015
26. Biradha K (2003) Crystal engineering: From weak hydrogen bonds to coordination bonds. Cryst Eng Comm 5(66):374–384
27. Filarowski A, Głowiaka T, Koll A (1999) Strengthening of the intramolecular O···H···N hydrogen bonds in Schiff bases as a result of steric repulsion. J Mol Struct 484(1–3):75–89
28. Tolstoy PM, Guo J, Koeppe B, Golubev NS, Denisov GS, Smirnov SN (2010) Geometries and tautomerism of OHN hydrogen bonds in aprotic solution probed by H/D isotope effects on 13C NMR chemical shifts. J Phys Chem A 114(40):10775–10782
29. Green J, Barnard P (1963) The vibrational frequencies of the ethylpyridines. J Chem Soc 640–643
30. Topaçlı A, Bayarı S (1999) Urey-Bradley force field of 4-ethylpyridine. Spectrochim Acta Part A: Mol Biomol Spect 55(7–8):1389–1394
31. Cummings D, Wood J (1974) The intermolecular force field of the hydrogen bond. J Mol Struct 20(1):1–40
32. Nakamoto K (2009) Infrared and Raman spectra of inorganic and coordination compounds, part B: applications in coordination, organometallic, and bioinorganic chemistry. Sixth ed. John Wiley & Sons
33. Balfour WJ, Ristic-Petrovic D (1993) Spectroscopic studies on the monobromotoluenes. J Phys Chem 97(45):11643–11648
34. Socrates G (2004) Infrared and Raman characteristic group frequencies: Tables and charts. Third ed. John Wiley & Sons